

# Translational symmetry broken magnetization plateau of the $S = 1$ antiferromagnetic Heisenberg chain with competing anisotropies

Tôru Sakai <sup>1,2</sup>, Kiyomi Okamoto,<sup>1</sup> Kouichi Okunishi <sup>3</sup>, Masaru Hashimoto,<sup>1</sup> Tomoki Houda,<sup>1</sup>  
Rito Furuchi,<sup>1</sup> and Hiroki Nakano<sup>1</sup>

<sup>1</sup>Graduate School of Science, University of Hyogo, Kouto 3-2-1, Kamigori, Ako-gun, Hyogo 678-1297, Japan

<sup>2</sup>National Institute for Quantum Science and Technology SPring-8, Kouto 1-1-1, Sayo, Sayo-gun, Hyogo 679-5148, Japan

<sup>3</sup>Department of Physics, Niigata University, Niigata 950-2181, Japan



(Received 26 August 2023; accepted 12 November 2023; published 22 November 2023)

We investigate the  $S = 1$  antiferromagnetic quantum spin chain with the exchange and single-ion anisotropies in a magnetic field, using numerical exact diagonalization of finite-size clusters, level spectroscopy analysis, and the density matrix renormalization group (DMRG). We find that a translational symmetry broken magnetization plateau possibly appears at the half of the saturation magnetization, when the anisotropies compete with each other. The level spectroscopy analysis gives the phase diagram at half the saturation magnetization. The DMRG calculation presents the magnetization curves for some typical parameters and clarifies the spin structure in the plateau phase.

DOI: [10.1103/PhysRevB.108.174435](https://doi.org/10.1103/PhysRevB.108.174435)

## I. INTRODUCTION

One-dimensional quantum spin systems have been attracting increasing attention both experimentally and theoretically in recent years [1]. Various kinds of phenomena that originate from strong spin-spin interactions as well as strong quantum fluctuations due to being in one dimension have been found. Among these phenomena, the magnetization plateau is one of most interesting phenomena because it is a macroscopic quantized phenomenon with a topological background in many-body spin systems. In quantum spin chains, based on the Lieb-Schultz-Mattis theorem [2], the rigorous necessary condition for the appearance of the plateau was derived as [3]

$$Q(S - \tilde{m}) = \text{integer}, \quad (1)$$

where  $S$  and  $\tilde{m}$  are the total spin and the magnetization per unit cell and  $Q$  is the periodicity of the ground state measured by the unit cell. The magnetization plateau for  $Q \geq 2$  should be accompanied by spontaneous translational symmetry breaking. The simple magnetization plateau for  $Q = 1$  has been theoretically predicted or experimentally observed in the following systems: the  $S = 3/2$  and  $S = 2$  anisotropic antiferromagnetic chains [4,5], the  $S = 1/2$  distorted diamond chain [6–14], the  $S = 1/2$  trimerized chain [15–19], the  $S = 1/2$  tetramerized chain [20–23], the  $S = 1/2$  two-leg ladder [24–27], the  $S = 1/2$  three-leg spin ladder and tube [28–32], the  $S = 1/2$  and  $S = 1$  skewed systems [33,34], the mixed spin chain [35–41], the  $p$ -leg ladder [28], and the polymerized chain [42,43].

For the  $S = 1$  chain case, when the unit cell is composed of one  $S = 1$  spin, the magnetization plateau at half of the saturation is impossible with  $Q = 1$  because Eq. (1) cannot be satisfied with  $S = 1$  and  $\tilde{m} = 1/2$ . Thus, the unit cell should be composed of two (more generally, an even number of)  $S = 1$  spins (namely, dimerization) for the realization of

this half plateau. In this case the parameter set  $S = 2$  and  $\tilde{m} = 1$  satisfies Eq. (1) with  $Q = 1$ . In fact, half magnetization plateaus were experimentally observed in several  $S = 1$  chain materials with dimerization [44,45]. A phase diagram on the plane of the dimerization parameter versus the magnetization was numerically obtained by Yan *et al.* [46].

The translational symmetry broken plateau for  $Q \geq 2$  also was revealed to appear in the following systems: the  $S = 1/2$  frustrated bond-alternating chain [47], the  $S = 1/2$  zigzag chain [48–50], the  $S = 1$  frustrated chain [51], the  $S = 1/2$  frustrated spin ladder [24–26,52–55], and the  $S = 1$  frustrated spin ladder [56–59]. In most cases, the mechanism of the  $Q \geq 2$  plateau has been based on the frustration. Recently, a numerical diagonalization study on the  $S = 2$  antiferromagnetic chain indicated that the competing anisotropies possibly yield the  $Q = 2$  plateau at half the saturation magnetization [60], as well as the  $Q = 1$  plateau. Thus, the competing anisotropies are expected to give rise to the  $Q = 2$  plateau, even without frustration.

However, the half magnetization plateau of the  $S = 1$  chain without dimerization (namely,  $Q = 2$ ,  $S = 1$ , and  $\tilde{m} = 1/2$ ) has not been observed so far [45] as far as we know. Thus, we think that it is important to clarify the condition for the realization of the half plateau in  $S = 1$  spin chains with  $Q = 2$ ,  $S = 1$ , and  $\tilde{m} = 1/2$ .

Considering the above situation, in this paper we investigate the  $S = 1$  antiferromagnetic chain with XXZ coupling and single-ion anisotropies competing with each other and clarify the condition for the  $Q = 2$  plateau at half the saturation magnetization. This may reveal the reason why such a plateau has not been experimentally observed, as well as provide a guide for finding or synthesizing materials showing such a plateau. Using numerical diagonalization of finite-size clusters and level spectroscopy analysis, the phase diagram at half the saturation magnetization is presented. In addition

the density matrix renormalization group (DMRG) calculation indicates that the  $Q = 2$  plateau actually appears on the magnetization curve. We also show the phase diagram of the magnetization process.

## II. MODEL

We investigate the magnetization process of the  $S = 1$  antiferromagnetic Heisenberg chain with the exchange and single-ion anisotropies, denoted by  $\lambda$  and  $D$ , respectively. The Hamiltonian is given by

$$\mathcal{H} = \mathcal{H}_0 + \mathcal{H}_Z, \quad (2)$$

$$\mathcal{H}_0 = \sum_{j=1}^L [S_j^x S_{j+1}^x + S_j^y S_{j+1}^y + \lambda S_j^z S_{j+1}^z] + D \sum_{j=1}^L (S_j^z)^2, \quad (3)$$

$$\mathcal{H}_Z = -H \sum_{j=1}^L S_j^z. \quad (4)$$

The exchange interaction constant is set to be unity as the unit of energy. For  $L$ -site systems, the lowest energy of  $\mathcal{H}_0$  in the subspace where  $\sum_j S_j^z = M$  is denoted as  $E(L, M)$ . The reduced magnetization  $m$  is defined as  $m = M/M_s$ , where  $M_s$  denotes the saturation of the magnetization, namely,  $M_s = L$ .  $E(L, M)$  is calculated by the Lanczos algorithm under the periodic boundary condition ( $S_{L+1} = S_1$ ). We consider the case in which  $\lambda$  is Ising-like and  $D$  is XY-like, namely,  $\lambda > 1$  and  $D > 0$ . Thus, easy-axis  $\lambda$  and easy-plane  $D$  compete with each other. If the magnetization plateau appears at  $m = 1/2$ , the translational symmetry should be spontaneously broken, and twofold degeneracy of the ground state should occur, namely,  $Q = 2$ .

## III. PHASE DIAGRAM AT $m = 1/2$

In this section using numerical diagonalization for finite-size clusters, the phenomenological renormalization group, and level spectroscopy analyses, we show that the magnetization plateau appears at  $m = 1/2$  for sufficiently large  $\lambda$  and  $D$  and present the phase diagram at  $m = 1/2$ .

### A. Phenomenological renormalization group

In order to confirm that the magnetization plateau really appears at  $m = 1/2$ , we apply the phenomenological renormalization group [61] for the plateau width  $W$ , defined as

$$W = E(L, M - 1) + E(L, M + 1) - 2E(L, M), \quad (5)$$

where  $M = L/2$ . Since  $W$  should be proportional to  $1/L$  in the no-plateau case, the scaled width  $LW$  should be independent of the system size  $L$ , while  $W$  should increase with  $L$  in the presence of a plateau. Let us set  $D = 5.0$  as an example. With fixed  $D = 5.0$ ,  $LW$  calculated for  $L = 10, 12, 14$ , and  $16$  is plotted versus  $\lambda$  in Fig. 1. Figure 1 shows that the plateau obviously appears for sufficiently large  $\lambda$ . However, it is difficult to determine the precise phase boundary with this method.

Next, we apply the phenomenological renormalization group analysis [61] for the excitation gap with momentum

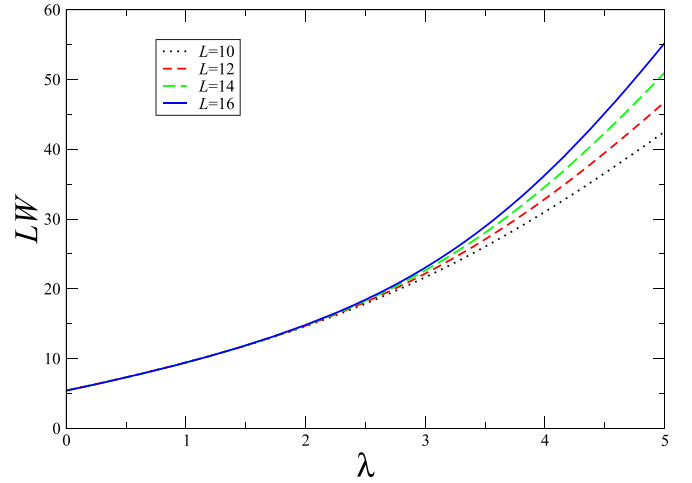


FIG. 1. Scaled plateau width  $LW$  plotted versus  $\lambda$  for  $L = 10, 12, 14$ , and  $16$  in the case of  $D = 5.0$ .

$k = \pi$  in the subspace  $m = 1/2$ , defined as  $\Delta_\pi$ . The size-dependent fixed point  $\lambda_c(L + 1)$  is determined by the equation

$$L\Delta_\pi(L, \lambda) = (L + 2)\Delta_\pi(L + 2, \lambda). \quad (6)$$

The scaled gaps  $L\Delta_\pi$  for  $D = 5.0$  are plotted versus  $\lambda$  for  $L = 10, 12, 14$ , and  $16$  in Fig. 2. The size-dependent fixed points  $\lambda_c(L)$  for  $L = 11, 13$ , and  $15$  are plotted versus  $1/L$  for  $D = 5.0$  in Fig. 3. The phase boundary in the thermodynamic limit is estimated as  $\lambda_c = 2.50 \pm 0.01$ . We repeat this procedure for various fixed  $D$  or for fixed  $\lambda$  to estimate the phase boundary. Actually, the phase boundary for  $D \geq 3.0$  was obtained using the fixed  $D$  method, while that for  $\lambda \geq 3.5$  is estimated using the  $\lambda$  method. The present result suggests that the translational symmetry is spontaneously broken and the ground state has a twofold degeneracy in the plateau phase. A Néel order like  $|\cdots 101010 \cdots\rangle$  is expected to be realized. Thus, we call this plateau the ‘‘Néel plateau.’’

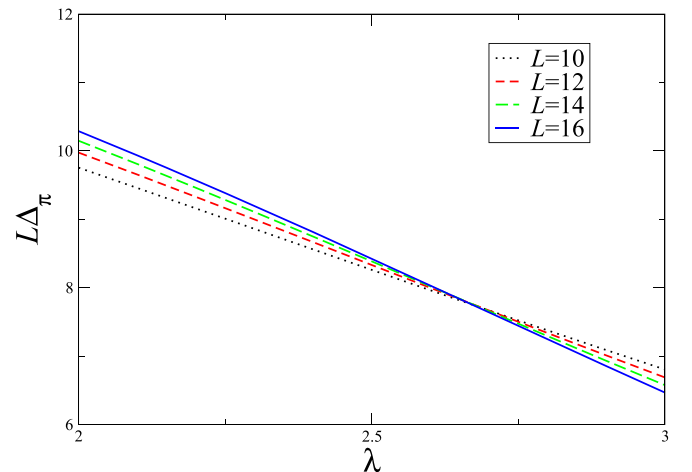


FIG. 2. Scaled gap  $L\Delta_\pi$  plotted versus  $\lambda$  for  $L = 10, 12, 14$ , and  $16$  in the case of  $D = 5.0$ .

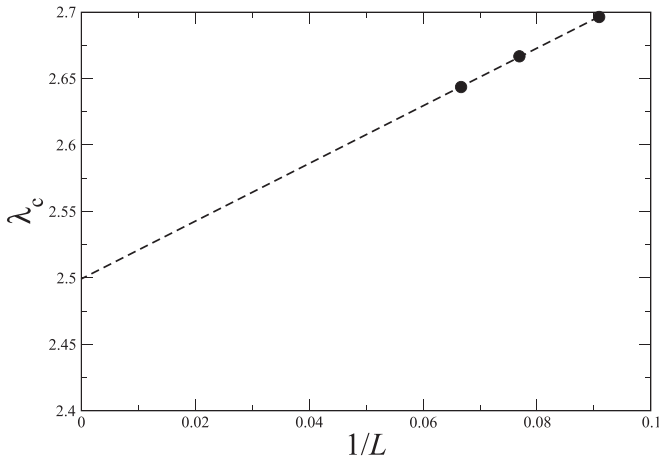


FIG. 3. Size-dependent fixed points  $\lambda_c(L)$  obtained using the phenomenological renormalization group method for  $L = 11, 13,$  and  $15$  are plotted versus  $1/L$  for  $D = 5.0$ . The phase boundary in the thermodynamic limit is estimated as  $\lambda_c = 2.50 \pm 0.01$ .

**B. Level spectroscopy**

One of the more precise methods to determine the phase boundary is level spectroscopy analysis [62,63]. Based on this method, comparing the single magnon excitation gap  $\Delta_1 \equiv W/2$  and  $\Delta_\pi$ , the gap  $\Delta_1$  is smaller in the no-plateau phase, while  $\Delta_\pi$  is smaller in the plateau phase. Thus,  $\Delta_1 = \Delta_\pi$  gives the size-dependent phase boundary.  $\Delta_1$  and  $\Delta_\pi$  for  $D = 5.0$  are plotted versus  $\lambda$  for  $L = 12, 14,$  and  $16$  in Fig. 4. Figure 4 shows the  $L$  dependence is quite small, and the size correction is predicted to be proportional to  $1/L^2$ . The extrapolation of  $\lambda_c$  to the thermodynamic limit gives  $\lambda_c = 2.401 \pm 0.001$ , as shown in Fig. 5. Although there is a small discrepancy in the extrapolated phase boundary between the phenomenological renormalization and the level spectroscopy because of a finite-size effect, the latter method is expected to be more precise because it is based on the essential nature of the Berezinskii-Kosterlitz-Thouless transition [1,62–66]. Namely, the lowest-order contributions of the logarithmic size

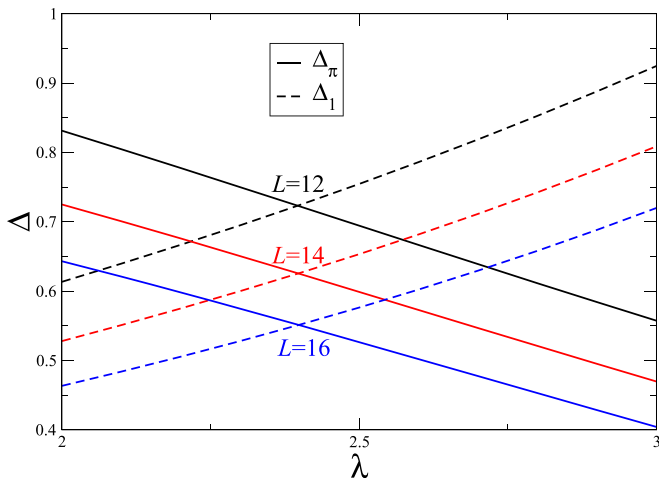


FIG. 4.  $\Delta_1$  and  $\Delta_\pi$  for  $D = 5.0$  are plotted versus  $\lambda$  for  $L = 12, 14,$  and  $16$ .

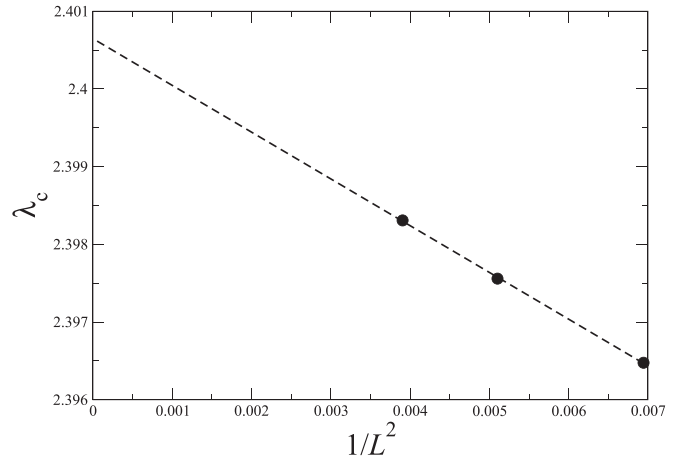


FIG. 5. The extrapolation of  $\lambda_c$  to the thermodynamic limit, assuming the size correction is proportional to  $1/L^2$ , gives  $\lambda_c = 2.401 \pm 0.001$ .

corrections each other out in the level spectroscopy method [62,63].

**C. Magnetization jump**

Apart from the no-plateau and magnetization plateau phases, there is a parameter region where the  $m = 1/2$  magnetization is not realized due to the magnetization jump, like the spin flop transition. A typical case for the “missing” region can be seen in the magnetization curve for  $\lambda = 8.0$  and  $D = 0.0$  in Fig. 8 below. There is a magnetization jump from about  $m = 0.04$  to  $m = 0.55$ , which means that the  $m = 1/2$  situation is not realized in this curve. If the  $m = 1/2$  magnetization is included in the magnetization jump, we say that the system is in the missing region. The boundary of the missing region  $D_m$  for  $\lambda = 8.0$  is plotted versus  $1/L$  in Fig. 6. Assuming the size correction is proportional to  $1/L$ ,  $D_m$  in the infinite-length

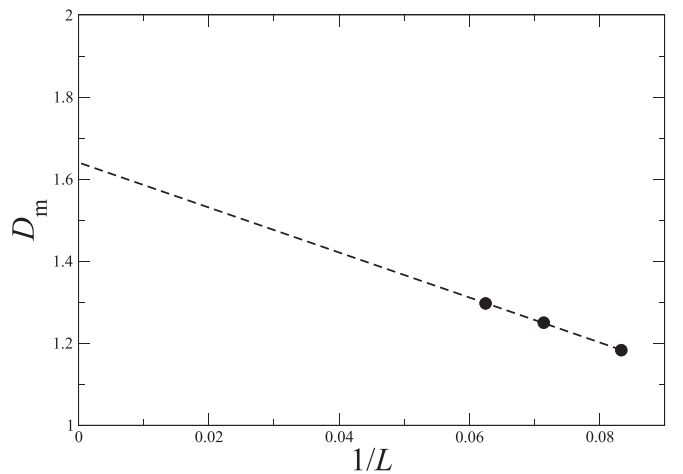


FIG. 6. The boundary of the missing region  $D_m$  for  $\lambda = 8.0$  is plotted versus  $1/L$ . Assuming the size correction is proportional to  $1/L$ ,  $D_m$  in the infinite-length limit is estimated as  $D_m = 1.64 \pm 0.01$ .

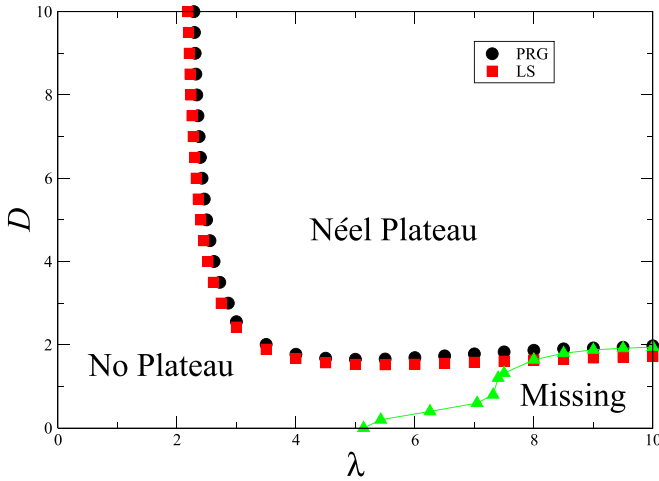


FIG. 7. Phase diagram at  $m = 1/2$  for the present model. The no-plateau and Néel plateau phases are shown, along with the missing region, which is surrounded by green triangles.

limit is estimated as  $D_m = 1.64 \pm 0.01$ . The boundary of the missing region is determined with this method.

#### D. Phase diagram

We present the phase diagram at half the saturation magnetization with respect to the easy-axis coupling anisotropy  $\lambda$  and the easy-plane single-ion one  $D$  in Fig. 7. It consists of the no-plateau and Néel plateau phases and the missing region, which is surrounded by green triangles. In the Néel plateau phase the translational symmetry is spontaneously broken, and  $Q = 2$  is realized.

#### IV. MAGNETIZATION CURVES

In order to confirm that the  $1/2$  magnetization plateau actually appears, we performed a DMRG calculation with  $L = 100$  to obtain the magnetization curves in the ground state. The calculated magnetization curves for  $(\lambda, D) = (4.0, 4.0)$ ,  $(5.0, 3.0)$ ,  $(6.0, 2.0)$ ,  $(7.0, 1.0)$ , and  $(8.0, 0.0)$  are shown in Fig. 8 by black circles, red squares, green pluses, blue crosses, and brown stars, respectively. The curves for  $(5.0, 3.0)$  and  $(6.0, 2.0)$  in the plateau phase obviously exhibit the  $1/2$  magnetization plateau. On the curve for  $(8.0, 0.0)$  the  $m = 1/2$  state is skipped due to the magnetization jump. For the case with  $(7.0, 1.0)$  the  $m = 1/2$  state is realized, although there is a magnetization jump.

The magnetization curves using the DMRG method for  $(\lambda, D) = (4.0, 4.0)$ ,  $(3.0, 5.0)$ ,  $(2.0, 6.0)$ ,  $(1.0, 7.0)$ , and  $(0.0, 8.0)$  are shown in Fig. 9 by black circles, red squares, green pluses, blue crosses, and brown stars, respectively. The curves for  $(0.0, 8.0)$ ,  $(1.0, 7.0)$ , and  $(2.0, 6.0)$  in the no-plateau phase have no plateau, while the ones for  $(3.0, 5.0)$  and  $(4.0, 4.0)$  in the plateau phase exhibit the  $1/2$  plateau. These magnetization curves are all consistent with the phase diagram in Fig. 7.

The saturation field  $H_s$  can be calculated from the energy difference between the energy of the ferromagnetic state and that of the one-spin-down state of the Hamiltonian (2).

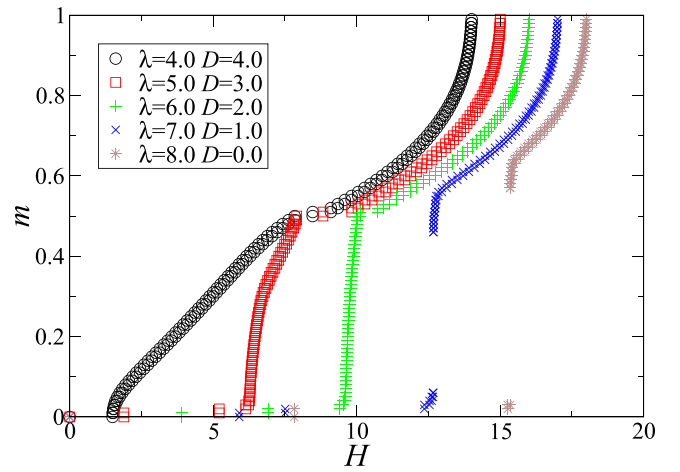


FIG. 8. The magnetization curves calculated by DMRG for  $(\lambda, D) = (4.0, 4.0)$ ,  $(5.0, 3.0)$ ,  $(6.0, 2.0)$ ,  $(7.0, 1.0)$ , and  $(8.0, 0.0)$  are shown by black circles, red squares, green pluses, blue crosses, and brown stars, respectively.

A simple calculation leads to

$$H_s = 2\lambda + D + 2. \quad (7)$$

All the magnetization curves in Figs. 8 and 9 were calculated under the condition  $\lambda + D = 8$ , which leads to

$$H_s = \lambda + 10. \quad (8)$$

This well explains all  $H_s$  in Figs. 8 and 9.

#### V. SPIN STRUCTURE

In order to investigate the spin structure at the  $1/2$  magnetization plateau, we calculated the magnetization at each site using the DMRG. The site magnetization  $\langle S_j^z \rangle$  at  $m = 1/2$  for  $(\lambda, D) = (4.0, 4.0)$  in the plateau phase is shown in Fig. 10. Figure 10 illustrates that the translational symmetry is

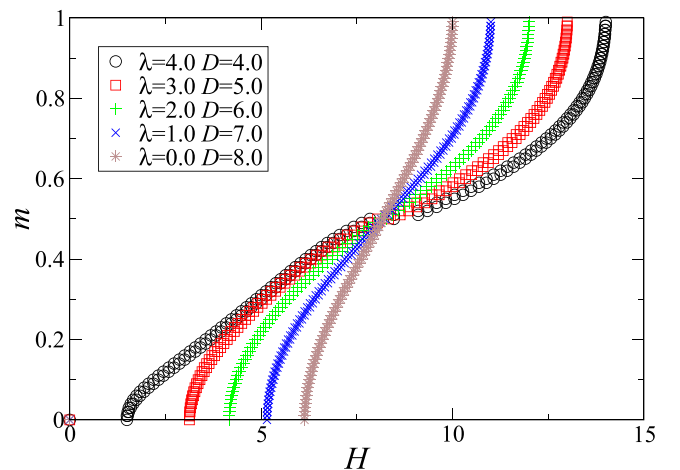


FIG. 9. The magnetization curves calculated by DMRG for  $(\lambda, D) = (4.0, 4.0)$ ,  $(3.0, 5.0)$ ,  $(2.0, 6.0)$ ,  $(1.0, 7.0)$ , and  $(0.0, 8.0)$  are shown by black circles, red squares, green pluses, blue crosses, and brown stars, respectively.

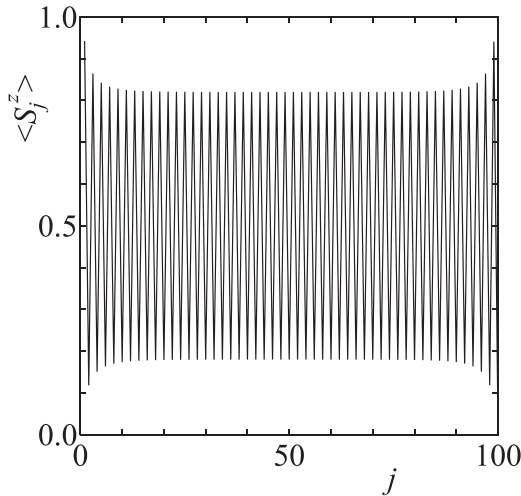


FIG. 10. Site magnetization  $\langle S_j^z \rangle$  for  $(\lambda, D) = (4.0, 4.0)$  in the Néel plateau phase by DMRG with  $L = 100$ . We can see the Néel-type structure  $|\cdots 101010 \cdots\rangle$ .

spontaneously broken and the periodicity  $Q = 2$  is realized. This is consistent with the physical picture of the Néel plateau.

## VI. EFFECTIVE THEORY

Let us start with the isolated spin limit to construct an effective theory. For the case of  $m = 1/2$ , the  $|S^z = 0\rangle$  state and the  $|S^z = 1\rangle$  state have the same energies, which are lower than the energy of the  $|S^z = -1\rangle$  state by  $2D$ . We can construct an effective theory by picking only the  $|S^z = 0\rangle$  state and the  $|S^z = 1\rangle$  state when  $D$  is sufficiently larger than the interactions, namely,

$$D \gg \lambda. \quad (9)$$

We introduce the pseudospin operator  $T$  with  $T = 1/2$ , where  $|T^z = 1/2\rangle$  and  $|T^z = -1/2\rangle$  represent  $|S^z = 1\rangle$  and  $|S^z = 0\rangle$ , respectively. In this restricted basis, we see

$$S^z = T^z + \frac{1}{2}, \quad S^\pm = \sqrt{2}T^\pm. \quad (10)$$

Therefore, we obtain the effective Hamiltonian:

$$\mathcal{H}_{\text{eff}} = \sum_{j=1}^L \{2(T_j^x T_{j+1}^x + T_j^y T_{j+1}^y) + \lambda T_j^z T_{j+1}^z\} + (\lambda + D - H) \sum_{j=1}^L T_j^z + L \frac{\lambda + D + H}{4}. \quad (11)$$

The condition  $\sum_j T_j^z = 0$  corresponds to  $m = 1/2$  of the original model. From the exact solution [1], the ground state of  $\mathcal{H}_{\text{eff}}$  for  $\sum_j T_j^z = 0$  is either the Tomonaga-Luttinger liquid state [1] (no plateau in the original model) or the Néel state (plateau with the Néel mechanism in the original model), depending on whether  $\lambda \leq 2$  or  $\lambda > 2$ . We note that there is a factor of 2 in front of  $T_j^x T_{j+1}^x + T_j^y T_{j+1}^y$  in Eq. (11). Thus, the behavior of the boundary between the plateau and no-plateau phases  $\lambda \rightarrow 2$  as  $D \rightarrow \infty$  in Fig. 7 is well explained. The magnetic field  $H_{1/2}$  corresponding to  $m = 1/2$  can be obtained

from the condition that the effective field for the  $T$  system is zero, namely,  $\lambda + D - H_{1/2} = 0$ , resulting in

$$H_{1/2} = \lambda + D. \quad (12)$$

For the magnetization curves in Figs. 8 and 9, we set  $\lambda + D = 8$ . Then DMRG results  $H_{1/2} \simeq 8$  for all the curves in Fig. 9 are also well explained by this effective theory. For the magnetization curves in Fig. 8, this effective theory does not hold because Eq. (9) is not satisfied.

In the phase diagram in Fig. 7, we see two features in the  $\lambda \rightarrow \infty$  limit. (i) The first is that the plateau-no-plateau line and the missing boundary line are going to merge, and (ii) the second is that the critical value of  $D$  tends to  $D_c \simeq 2$ . Liu *et al.* [67] investigated the phase diagram of the  $S = 1$  Ising chain

$$\mathcal{H} = \sum_{j=1}^L S_j^z S_{j+1}^z + D_0 \sum_{j=1}^L (S_j^z)^2 - H \sum_{j=1}^L S_j^z \quad (13)$$

to obtain the phase diagram on the  $D_0$ - $H$  plane. Feature (i) is consistent with the phase diagram of Liu *et al.*, but feature (ii) cannot be explained by it since the transverse coupling is not included their Hamiltonian (13).

## VII. PHASE DIAGRAM OF THE MAGNETIZATION PROCESS

In order to consider some realistic experiments, it would be useful to obtain the phase diagram of the magnetization process summarizing the spin structure. In the gapless phase of the magnetization process, the system is expected to be in the Tomonaga-Luttinger liquid phase. It is characterized by the power-law decay of the spin correlation functions, which have the asymptotic forms

$$\langle S_0^z S_r^z \rangle - m^2 \sim \cos(2k_F r) r^{-\eta_z}, \quad (14)$$

$$\langle S_0^x S_r^x \rangle \sim (-1)^r r^{-\eta_x} \quad (15)$$

in the infinite- $r$  limit.  $2k_F$  is  $\pi(1 - m)$  in the present model. The first equation corresponds to the spin density wave (SDW) spin correlation parallel to the external field, and the second one corresponds to the Néel-like spin correlation perpendicular to the external field. The smaller exponent between  $\eta_z$  and  $\eta_x$  determines the dominant spin correlation. In the conventional magnetization process the canted Néel-like spin correlation is dominant, namely,  $\eta_x < \eta_z$ . However, in some frustrated systems the magnetization region where  $\eta_z < \eta_x$  is realized appears, and the incommensurate spin correlation parallel to the external field is dominant there [68]. Then we consider the possibility of a similar interesting behavior in the present model. According to the conformal field theory, these exponents can be estimated by [69]

$$\eta_x = \frac{E(L, M + 1) + E(L, M - 1) - 2E(L, M)}{E_{k_1}(L, M) - E(L, M)}, \quad (16)$$

$$\eta_z = 2 \frac{E_{2k_F}(L, M) - E(L, M)}{E_{k_1}(L, M) - E(L, M)} \quad (17)$$

for each magnetization  $M$ , where  $k_1$  is defined as  $k_1 = L/2\pi$ . Since the relation  $\eta_x \eta_z = 1$  is satisfied in the

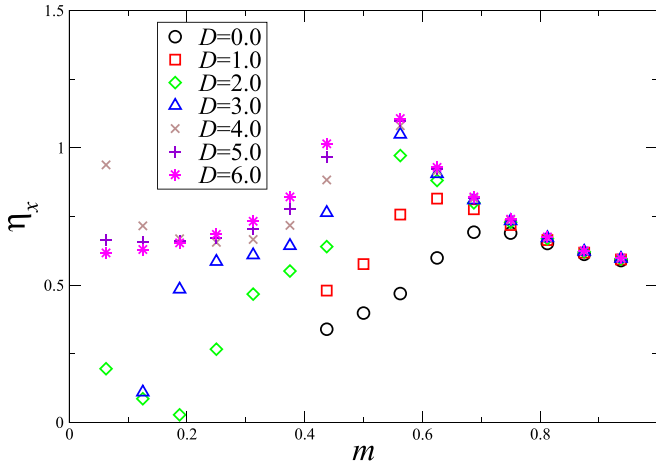


FIG. 11. Exponent  $\eta_x$  estimated by the numerical exact diagonalization of the 16-spin system for  $\lambda = 4.0$  plotted versus  $m$  for  $D = 0.0$  (black circles), 1.0 (red squares), 2.0 (green diamonds), 3.0 (blue triangles), 4.0 (brown crosses), 5.0 (violet pluses), and 6.0 (pink stars).

Tomonaga-Luttinger liquid phase, we have to calculate only one of these two exponents to determine the dominant spin correlation. We estimate the exponent  $\eta_x$  here because the calculation of  $\eta_z$  meets the larger finite-size correlation due to the incommensurate correlation expressed by the cosine factor in Eq. (15). The estimated exponent  $\eta_x$  from the numerical exact diagonalization for  $L = 16$  and  $\lambda = 4.0$  is plotted versus the magnetization  $m$  for several values of  $D$  in Fig. 11. In the case of  $D \geq 3.0$ , the magnetization region where  $\eta_x$  is larger than 1 appears around  $m \sim 1/2$ . This indicates that the  $z$  component dominant Tomonaga-Luttinger liquid phase takes place. Using the numerical exact diagonalization for  $L = 16$ ,  $\eta_x$  can be calculated for  $M = 1, 2, \dots, 15$ . Then we estimate the crossover line  $\eta_x = 1$ , linearly interpolating the calculated values of  $\eta_x$  at  $M$  and  $M + 1$  between which  $\eta_x = 1$  would occur. In addition, we estimate the critical point  $D_c$  where the magnetization jump begins at each  $M$  using the numerical exact diagonalization for  $L = 16$ . The estimated crossover line between the  $z$  component dominant Tomonaga-Luttinger liquid ( $z$ TLL) phase and the  $xy$  component dominant one ( $xy$ TLL) and the critical line of the magnetization jump are shown in the  $D$  and magnetization phase diagram for  $\lambda = 4.0$  in Fig. 12. In order to confirm whether the crossover line really exists even in the thermodynamic limit, we also calculate  $\langle S_j^x S_{j+r}^x \rangle$  for the central region of an  $L = 100$  chain with DMRG and then estimate the exponent of its power-law decay for  $r = 1-30$ . The crossover lines estimated by the numerical exact diagonalization and by the DMRG are shown as blue crosses and blue circles, respectively, in Fig. 12. They are consistent with each other, which suggests that the  $z$ TLL phase is realized even in the infinite-length limit. In conclusion, it is found that the present competing anisotropies give rise to the  $1/2$  translational symmetry broken magnetization plateau and the incommensurate parallel spin correlation dominant Tomonaga-Luttinger liquid ( $z$ TLL) phase around the plateau. Even for different  $\lambda$ , qualitatively similar phase diagrams would be obtained.

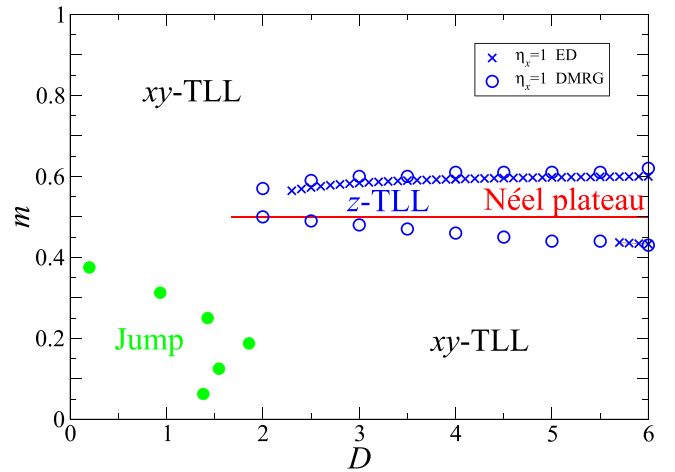


FIG. 12. Phase diagram with respect to the anisotropy  $D$  and the magnetization  $m$ . The crossover lines between the incommensurate parallel spin correlation dominant Tomonaga-Luttinger liquid ( $z$ TLL) phase and the Néel-like perpendicular correlation dominant one ( $xy$ TLL) are estimated using the numerical exact diagonalization (ED; blue crosses) and the DMRG (blue circles). The phase boundary of the missing region that results from the magnetization jump is estimated using numerical exact diagonalization for  $L = 16$  (green circles). The Néel plateau is realized just on the red line.

## VIII. SUMMARY

The magnetization process of the  $S = 1$  antiferromagnetic chain with easy-axis coupling anisotropy and easy-plane single-ion anisotropy was investigated using numerical diagonalization for finite-size clusters and DMRG calculations. It was found that the translational symmetry broken magnetization plateau appears at half the saturation magnetization for very large anisotropies (both of  $\lambda$  and  $D$ ). This explains why this plateau has not yet been found in the  $S = 1$  chain compounds without dimerization [45]. Several typical magnetization curves were also presented. Thus, the effective theory constructed for  $D \gg \lambda$  well explains the numerical results in Fig. 7. Nevertheless, an effective theory for the  $D \ll \lambda$  case and the magnetization jump is a future problem. In addition, it was shown that the unconventional incommensurate parallel spin correlation dominant ( $\eta_x > \eta_z$ ) Tomonaga-Luttinger liquid phase also appears around the  $1/2$  plateau as in Fig. 12. This situation is very natural because the condition for the realization [1] of the Néel state ( $|\dots 101010 \dots\rangle$ ) is both  $\eta_x > \eta_z$  and the commensurability, which is satisfied only at  $m = 1/2$ .

In a previous work [60] we investigated the half-plateau problem of a similar model but with  $S = 2$  to obtain the phase diagram, which was much richer than Fig. 7 in this paper. In fact, the Haldane plateau phase and the large- $D$  plateau phase appeared in the  $S = 2$  case. This is because the half plateau is possible without spontaneous breaking of the translational symmetry for the  $S = 2$  case. Namely, the condition (1) can be satisfied by  $Q = 1$ ,  $S = 2$ , and  $\tilde{m} = 1$  (note that  $\tilde{m} = 1$  for the half plateau of the  $S = 2$  chain).

From the experimental point of view, one can usually expect a weak interchain interaction, which may induce the spin order corresponding to the most dominant correlation at a low,

but finite, temperature. The phase diagram in Fig. 12 suggests that the incommensurate-SDW order associated with the  $z$ TLL can be realized around the  $m = 1/2$  plateau in the broad parameter region. Thus, such an enhancement of the SDW order could be a signature of the  $m = 1/2$  plateau due to the Néel-type mechanism, even if the width of the plateau is very narrow. We believe that the phase diagrams in Figs. 7 and 12 will be a powerful guideline for searching for or synthesizing quasi-one-dimensional materials with  $S = 1$  which exhibit the half plateau without dimerization.

#### ACKNOWLEDGMENTS

This work was partly supported by KAKENHI, Grants No. JP16K05419, No. JP20K03866, No. JP16H01080

(J-Physics), No. JP18H04330 (J-Physics), No. JP20H05274, and No. 23K11125 from JSPS of Japan, and also by a Grant-in-Aid for Transformative Research Areas “The Natural Laws of Extreme Universe—A New Paradigm for Spacetime and Matter from Quantum Information” (KAKENHI Grant No. JP21H05191) from MEXT of Japan. Some of the computations were performed using facilities of the Supercomputer Center, Institute for Solid State Physics, University of Tokyo, and the Computer Room, Yukawa Institute for Theoretical Physics, Kyoto University. We used the computational resources of the supercomputer Fugaku provided by RIKEN through the HPCI System Research projects (Projects No. hp200173, No. hp210068, No. hp210127, No. hp210201, No. hp220043, and No. hp230114).

- 
- [1] For a review, see T. Giamarchi, *Quantum Physics in One Dimension* (Clarendon, Oxford, 2003).
- [2] E. H. Lieb, T. Schultz, and D. J. Mattis, *Ann. Phys. (NY)* **16**, 407 (1961).
- [3] M. Oshikawa, M. Yamanaka, and I. Affleck, *Phys. Rev. Lett.* **78**, 1984 (1997).
- [4] T. Sakai and M. Takahashi, *Phys. Rev. B* **42**, 4537 (1990).
- [5] A. Kitazawa and K. Okamoto, *Phys. Rev. B* **62**, 940 (2000).
- [6] A. Honecker and A. Läuchli, *Phys. Rev. B* **63**, 174407 (2001).
- [7] K. Okamoto, T. Tonegawa, and M. Kaburagi, *J. Phys.: Condens. Matter* **15**, 5979 (2003).
- [8] H. Kikuchi, Y. Fujii, M. Chiba, S. Mitsudo, T. Idehara, T. Tonegawa, K. Okamoto, T. Sakai, T. Kuwai, and H. Ohta, *Phys. Rev. Lett.* **94**, 227201 (2005).
- [9] B. Gu and G. Su, *Phys. Rev. B* **75**, 174437 (2007).
- [10] A. Honecker, S. Hu, R. Peters, and J. Richter, *J. Phys.: Condens. Matter* **23**, 164211 (2011).
- [11] N. S. Ananikian, J. Strečka, and V. Hovhannisyan, *Solid State Commun.* **194**, 48 (2014).
- [12] K. Morita, M. Fujihala, H. Koorikawa, T. Sugimoto, S. Sota, S. Mitsuda, and T. Tohyama, *Phys. Rev. B* **95**, 184412 (2017).
- [13] Y. Ueno, T. Zenda, Y. Tachibana, K. Okamoto, and T. Sakai, *JPS Conf. Proc.* **30**, 011085 (2020).
- [14] R. R. Montenegro-Filho, F. S. Matias, and M. D. Coutinho-Filho, *Phys. Rev. B* **102**, 035137 (2020).
- [15] K. Hida, *J. Phys. Soc. Jpn.* **63**, 2359 (1994).
- [16] K. Okamoto, *Solid State Commun.* **98**, 245 (1996).
- [17] K. Okamoto and A. Kitazawa, *J. Phys. A* **32**, 4601 (1999).
- [18] S.-S. Gong, B. Gu, and G. Su, *Phys. Lett. A* **372**, 2322 (2008).
- [19] G.-H. Liu, W. Li, W.-L. You, G. Su, and G.-S. Tian, *J. Magn. Magn. Mater.* **377**, 12 (2015).
- [20] S.-S. Gong and G. Su, *Phys. Rev. B* **78**, 104416 (2008).
- [21] S. Mahdaviifar and J. Abouie, *J. Phys.: Condens. Matter* **23**, 246002 (2011).
- [22] J.-J. Jiang, Y.-J. Liu, F. Tang, C.-H. Yang, and Y.-B. Sheng, *Commun. Theor. Phys.* **61**, 1 (2014).
- [23] X.-Y. Deng, J.-Y. Dou, and G.-H. Liu, *J. Magn. Magn. Mater.* **392**, 56 (2015).
- [24] T. Sugimoto, M. Mori, T. Tohyama, and S. Maekawa, *Phys. Rev. B* **97**, 144424 (2018).
- [25] T. Sugimoto, M. Mori, T. Tohyama, and S. Maekawa, *Phys. Rev. B* **92**, 125114 (2015).
- [26] K. Sasaki, T. Sugimoto, T. Tohyama, and S. Sota, *Phys. Rev. B* **101**, 144407 (2020).
- [27] Sk. S. Rahaman, M. Kumar, and S. Sahoo, [arXiv:2304.12266](https://arxiv.org/abs/2304.12266).
- [28] D. C. Cabra, A. Honecker, and P. Pujol, *Phys. Rev. Lett.* **79**, 5126 (1997).
- [29] K. Okamoto, M. Sato, K. Okunishi, T. Sakai, and C. Itoi, *Phys. E (Amsterdam, Neth.)* **43**, 769 (2011).
- [30] R. Li, S.-L. Wang, Y. Ni, K.-L. Yao, and H.-H. Fu, *Phys. Lett. A* **378**, 970 (2014).
- [31] R. C. Alcício, M. L. Lyra, and J. Strečka, *J. Magn. Magn. Mater.* **417**, 294 (2016).
- [32] A. Farchakh, A. Boubekri, and M. El Hafidi, *J. Low Temp. Phys.* **206**, 131 (2022).
- [33] L. Yin, Z. W. Ouyang, J. F. Wang, X. Y. Yue, R. Chen, Z. Z. He, Z. X. Wang, Z. C. Xia, and Y. Liu, *Phys. Rev. B* **99**, 134434 (2019).
- [34] D. Dey, S. Das, M. Kumar, and S. Ramasesha, *Phys. Rev. B* **101**, 195110 (2020).
- [35] S. Yamamoto and T. Sakai, *Phys. Rev. B* **62**, 3795 (2000).
- [36] T. Sakai and K. Okamoto, *Phys. Rev. B* **65**, 214403 (2002).
- [37] T. Tonegawa, T. Sakai, K. Okamoto, and M. Kaburagi, *J. Phys. Soc. Jpn.* **76**, 124701 (2007).
- [38] A. S. F. Tenório, R. R. Montenegro-Filho, and M. D. Coutinho-Filho, *J. Phys.: Condens. Matter* **23**, 506003 (2011).
- [39] G.-H. Liu, L.-J. Kong, and J.-Y. Dou, *Solid State Commun.* **213–214**, 10 (2015).
- [40] K. Karlova and J. Strečka, *Phys. B (Amsterdam, Neth.)* **536**, 494 (2018).
- [41] H. Yamaguchi, T. Okita, Y. Iwasaki, Y. Kono, N. Uemoto, Y. Hosokoshi, T. Kida, T. Kawakami, A. Matsuo, and M. Hagiwara, *Sci. Rep.* **10**, 9193 (2020).
- [42] D. C. Cabra, A. De Martino, A. Honecker, P. Pujol, and P. Simon, *Phys. Lett. A* **268**, 418 (2000).
- [43] W. Chen, K. Hida, and B. C. Sanctuary, *Phys. Rev. B* **63**, 134427 (2001).
- [44] Y. Narumi, K. Kindo, M. Hagiwara, H. Nakano, A. Kawaguchi, K. Okunishi, and M. Kohno, *Phys. Rev. B* **69**, 174405 (2004).
- [45] For a review of  $S = 1$  chain compounds, see O. V. Maximova, S. V. Streltsov, and A. N. Vasiliev, *Crit. Rev. Solid State Mater. Sci.* **46**, 371 (2021).
- [46] X. Yan, W. Li, Y. Zhao, S.-J. Ran, and G. Su, *Phys. Rev. B* **85**, 134425 (2012).

- [47] K. Totsuka, *Phys. Rev. B* **57**, 3454 (1998).
- [48] K. Okunishi and T. Tonegawa, *J. Phys. Soc. Jpn.* **72**, 479 (2003).
- [49] K. Okunishi and T. Tonegawa, *Phys. Rev. B* **68**, 224422 (2003).
- [50] A. Metavitsiadis, C. Psaroudaki, and W. Brenig, *Phys. Rev. B* **101**, 235143 (2020).
- [51] H. Nakano and M. Takahashi, *J. Phys. Soc. Jpn.* **67**, 1126 (1998).
- [52] N. Okazaki, J. Miyoshi, and T. Sakai, *J. Phys. Soc. Jpn.* **69**, 37 (2000).
- [53] N. Okazaki, K. Okamoto, and T. Sakai, *J. Phys. Soc. Jpn.* **69**, 2419 (2000).
- [54] A. Nakasu, K. Totsuka, Y. Hasegawa, K. Okamoto, and T. Sakai, *J. Phys.: Condens. Matter* **13**, 7421 (2001).
- [55] T. Sakai and Y. Hasegawa, *Phys. Rev. B* **60**, 48 (1999).
- [56] K. Okamoto, N. Okazaki, and T. Sakai, *J. Phys. Soc. Jpn.* **70**, 636 (2001).
- [57] K. Okamoto, N. Okazaki, and T. Sakai, *J. Phys. Soc. Jpn.* **71**, 196 (2002).
- [58] F. Michaud, T. Coletta, S. R. Manmana, J.-D. Picon, and F. Mila, *Phys. Rev. B* **81**, 014407 (2010).
- [59] H. Kohshiro, R. Kaneko, S. Morita, H. Katsura, and N. Kawashima, *Phys. Rev. B* **104**, 214409 (2021).
- [60] T. Yamada, R. Nakanishi, R. Furuchi, H. Nakano, H. Kaneyasu, K. Okamoto, T. Tonegawa, and T. Sakai, *JPS Conf. Proc.* **38**, 011163 (2023).
- [61] M. P. Nightingale, *Physica A (Amsterdam, Neth.)* **83**, 561 (1976).
- [62] K. Okamoto and K. Nomura, *Phys. Lett. A* **169**, 433 (1992).
- [63] K. Nomura and K. Okamoto, *J. Phys. A* **27**, 5773 (1994).
- [64] Z. L. Berezinskii, *Sov. Phys. JETP* **34**, 610 (1971).
- [65] J. M. Kosterlitz and D. J. Thouless, *J. Phys. C* **6**, 1181 (1973).
- [66] J. V. José, *40 Years of Berezinskii-Kosterlitz-Thouless Theory* (World Scientific, Singapore, 2013).
- [67] G.-H. Liu, W. Li, W.-L. You, G. Su, and G.-S. Tian, *Solid State Commun.* **166**, 38 (2013).
- [68] N. Maeshima, K. Okunishi, K. Okamoto, and T. Sakai, *Phys. Rev. Lett.* **93**, 127203 (2004).
- [69] J. L. Cardy, *J. Phys. A* **17**, L385 (1984).